JOURNAL OF VIROLOGY, Sept. 1995, p. 5475–5484 Vol. 69, No. 9
0022-538X/95/$04.00+0


# Construction of Murine Coronavirus Mutants Containing Interspecies Chimeric Nucleocapsid Proteins

DING PENG,[1]† CHERI A. KOETZNER,[2] TIMOTHY McMAHON,[1] YUAO ZHU,[1] AND PAUL S. MASTERS[1,2]*

*Department of Biomedical Sciences, State University of New York at Albany,[1] and Wadsworth Center for Laboratories and Research, New York State Department of Health,[2] Albany, New York*

Received 21 April 1995/Accepted 7 June 1995

**Targeted RNA recombination was used to construct mouse hepatitis virus (MHV) mutants containing chimeric nucleocapsid (N) protein genes in which segments of the bovine coronavirus N gene were substituted in place of their corresponding MHV sequences. This defined portions of the two N proteins that, despite evolutionary divergence, have remained functionally equivalent. These regions included most of the centrally located RNA-binding domain and two putative spacers that link the three domains of the N protein. By contrast, the amino terminus of N, the acidic carboxy-terminal domain, and a serine- and arginine-rich segment of the central domain could not be transferred from bovine coronavirus to MHV, presumably because these parts of the molecule participate in protein-protein interactions that are specific for each virus (or, possibly, each host). Our results demonstrate that targeted recombination can be used to make extensive substitutions in the coronavirus genome and can generate recombinants that could not otherwise be made between two viruses separated by a species barrier. The implications of these findings for N protein structure and function as well as for coronavirus RNA recombination are discussed.**

The nucleocapsid protein (N) of coronaviruses is intrinsic to a number of interesting properties of this family of viruses. Multiple monomers of N coat the uniquely large (26- to 31-kb), nonsegmented RNA coronavirus genome, and this ribonucleoprotein complex constitutes the only internal component of the membrane-enclosed virion (38, 42). Coronavirus nucleocapsids have helical, rather than icosahedral symmetry, which makes them unusual among positive-sense RNA viruses. This characteristic poses important questions as to how the viral RNA is uncoated in the earliest steps of infection to allow translation of the genome and how progeny genomes are assembled into virions late in infection. The only known post-translational modification of N, phosphorylation, is an attractive candidate for a regulator of these events (39–41). However, it has not been established whether N phosphorylation is a dynamic process or which of the many serine residues of the molecule are its targets. There is some evidence suggesting roles for N in viral RNA synthesis (5, 7) as well as in translation of viral mRNAs (43), but these remain to be more clearly elucidated.

We previously sought to obtain structural information about the N protein of mouse hepatitis virus (MHV), an exemplar of this virus family, by comparing the sequences of the N genes of five strains of MHV (31). This led us to propose a model for N protein that consisted of three highly conserved domains separated by linkers (spacers A and B) that had diverged considerably among different strains. The first two domains are highly basic; the small, carboxy-terminal domain III is the only acidic portion of the molecule. N protein sequences subsequently reported for four additional MHV strains were fully in accord with this picture (9, 23, 24). The RNA-binding property of MHV N has been independently mapped by two groups to be within the middle domain (domain II) (27, 30). Beyond the fact that they are dispensable with respect to RNA binding, the function(s) of domains I and III are unknown.

Partial support for the model came from the identification of an MHV N gene mutant (Alb4) containing a deletion encompassing spacer B (21). The viability of this virus under permissive conditions established that spacer B was nonessential. Twelve second-site revertants of Alb4 were isolated, and all contained single amino acid changes in domain II (33). Two types of these mutations that were examined in detail were found to cause N protein to bind more tightly to RNA than wild-type N.

Although the interstrain sequence comparison was a useful starting point for examination of N, it was limited by the high homology (>90%) among all of the MHV N proteins. We sought to extend this analysis to a more distant relative of MHV, bovine coronavirus (BCV), since its N gene and N protein have 70% sequence homology to those of MHV (26). This required knowledge of which portions of the two heterologous N proteins were functionally equivalent, information that could not be obtained by classical genetic methods owing to the stringent species specificities exhibited by coronaviruses (8, 38, 42). One distinguishing feature of coronaviruses, their extraordinary genome size, poses an obstacle to genetic manipulation which we have addressed by exploiting another distinguishing feature of these viruses, their high rate of homologous RNA recombination (25). We have previously shown that it is possible to incorporate site-specific mutations into the N gene and the 3′ untranslated region of MHV by transfecting synthetic subgenomic or defective interfering (DI) RNA into infected cells to repair a selectable marker by RNA recombination (21, 28, 33). In an attempt to further our understanding of MHV N protein structure and function, and also to test the limits of targeted recombination mutagenesis, we set out to examine the possibility of substituting portions of the coding region of the MHV N protein with the corresponding regions of the BCV N protein.

* Corresponding author. Mailing address: Wadsworth Center, New York State Department of Health, New Scotland Ave., P.O. Box 22002, Albany, NY 12201-2002. Phone: (518) 474-1283. Fax: (518) 473-1326.

† Present address: Memorial Sloan Kettering Cancer Center, New York, NY 10021.

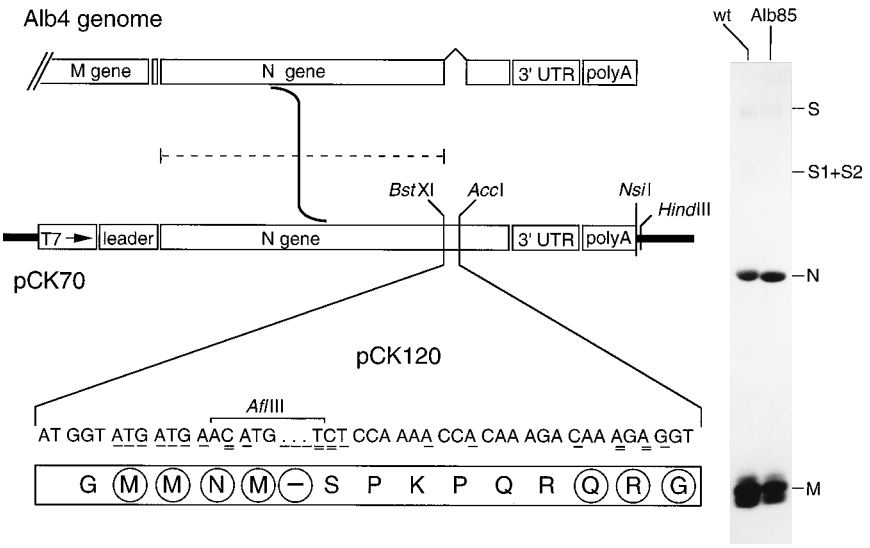


FIG. 1. Substitution of a portion of the spacer B region of the MHV N protein with its counterpart from the BCV N protein by targeted recombination. Vector pCK120 was constructed from pCK70, a template for in vitro transcription of MHV subgenomic RNA7 (21). The *Bst*XI-*Acc*I fragment of pCK70 was replaced with a *Bst*XI-*Acc*I oligonucleotide cassette encoding the first half of the BCV spacer B region. The sequence of the upper oligonucleotide is shown. Nonunderlined bases are the same as those in MHV; bases with a single underline are the same as those in BCV but differ from those in MHV; bases with a double underline differ from both those in BCV and those in MHV. A newly created *Afl*III site is indicated. In the translation product below, circled amino acids are those that are the same as those in BCV but differ from those in MHV; other amino acids are identical to those in BCV and MHV. Dashed line above the vector, region in which a crossover event between vector-derived synthetic RNA and Alb4 genomic RNA could have generated the selected recombinants. Structural proteins of recombinant Alb85 and wild-type (wt) virions are shown on the right. Viruses were radiolabeled with [$^{35}$S]methionine from 1 to 22 h postinfection and purified on potassium tartrate-glycerol gradients, as described previously (21). Equal amounts of each virus, as determined by protein concentration, were analyzed by SDS-PAGE followed by fluorography. UTR, untranslated region.

## MATERIALS AND METHODS

**Virus and cells.** MHV-A59 wild-type, mutant Alb1 and Alb4, and recombinant viruses were propagated in mouse 17Cl1 cells. Plaque titrations and plaque purifications were performed in mouse L2 cells. Spinner cultures of L2 cells, used for transfection by electroporation, were maintained as described previously (28).

**Plasmid constructs.** Vectors for the transcription of chimeric N genes were constructed either from pCK70, which encodes a copy of MHV subgenomic RNA7 (21), or from pB36, which encodes a synthetic DI RNA containing the entire MHV N gene (28). DNA was manipulated by standard methods (35); all newly generated junctions and PCR-created segments were verified by sequencing.

A vector, pCK120, substituting a portion of the MHV N gene spacer B region with material equivalent to the corresponding segment of the BCV N gene spacer B, was constructed by replacement of the *Bst*XI-*Acc*I fragment of pCK70 with a cassette made from two oligonucleotides, PM171 and PM172 (Fig. 1; Table 1). The oligonucleotide cassette was 3 bp smaller than the fragment that it replaced, owing to a single-amino-acid gap in the alignment of the two sequences in this region. In addition, the oligonucleotide cassette was designed to include a new *Afl*III site for the purposes of PCR analysis and of making further constructs. The protein encoded by pCK120 replaced amino acids 384 to 397 of the MHV N protein with amino acids 386 to 398 of the BCV N protein (26).

A vector, pTM1, substituting the entirety of domains I and II in addition to a portion of spacer B of the MHV N gene with the corresponding regions of the BCV N gene, was constructed through a series of intermediates (Fig. 2). The first of these was pB11, containing the entire BCV N gene and 3′ untranslated region attached to the MHV leader region from pCK70. A perfect junction between the MHV leader and the 5′ end of the BCV N coding region was generated by splicing overlap extension (SOE) PCR (14) using inside primers PM180 and PM181 and external primers PM179 and PM182 (Table 1). Initially, PM179 and PM180 were used to amplify the MHV leader from pCK70; PM181 and PM182 were used to amplify the beginning of the BCV N coding region from plasmid pLN (13) (generously provided by David Brian and Savithra Senanayake, University of Tennessee). The PCR fragments produced were then purified, mixed, and amplified with PM179 and PM182. The resulting PCR fragment was restricted with *Bam*HI and *Sac*I and assembled into pB11 via a three-way ligation with the vector *Bam*HI-*Hin*dIII fragment of pCK70 and the remainder of the BCV N gene contained in the *Sac*I-*Hin*dIII fragment of pLN. The MHV N gene domain III was then restored to pB11 in a three-way ligation consisting of the *Nsi*I-*Hin*dIII fragment of pB11 and the *Afl*III-*Hin*dIII fragment of pCK120 linked with an *Nsi*I-*Afl*III cassette made from oligonucleotides PM186 and PM187 (Table 1). The resulting construct was pB20.

The chimeric N coding region of pB20 was finally transferred to pB36. Plasmid pB36 encodes an MHV DI RNA in which the N gene forms a continuous open reading frame with the start of the gene 1 protein (28). A *Bam*HI site was added immediately prior to the start codon of the BCV N gene by PCR with primers PM194A and PM182 (Table 1) on pB20. The PCR product was restricted with *Bam*HI and *Xba*I and joined with the *Xba*I-*Bsi*WI fragment of pB20 and the *Bsi*WI-*Bam*HI fragment of pB36 in a three-way ligation to yield pTM1. The protein encoded by pTM1 replaced amino acids 1 to 397 of the MHV N protein with amino acids 1 to 398 of the BCV N protein. At its amino terminus, the encoded chimeric N protein was fused, in frame, to the first 86 amino acids of the MHV gene 1 protein product with one intervening heterologous residue.

Three additional vectors containing different combinations of the MHV and BCV N genes were subsequently constructed (see Fig. 4). Plasmid pP20, derived from pTM1, was made by substituting the *Bsu*36I-*Spe*I fragment of pTM1 with the equivalent fragment from pB36. The protein encoded by pP20 replaced amino acids 1 to 187 and 307 to 397 of the MHV N protein with amino acids 1 to 184 and 306 to 398 of the BCV N protein. Plasmid pP22, a vector containing the coding region for the carboxy-terminal portion of the BCV N protein, was made by replacing the *Spe*I-blunted *Bst*EII fragment of pB36 with the corresponding *Spe*I-blunted *Dra*III fragment of pLN. The protein encoded by pP22 replaced amino acids 307 to 454 of the MHV N protein with amino acids 306 to 448 of the BCV N protein. Plasmid pP24, a vector with all of the BCV N coding region, was made by inserting the *Spe*I-blunted *Dra*III fragment of pLN in place of the *Spe*I-blunted *Bst*EII fragment of pTM1. The protein encoded by pP24 replaced the entire 454 amino acids of the MHV N protein with the entire 448 amino acids of the BCV N protein.

**Targeted recombination.** Various extents of the BCV N coding region were transduced into MHV by the targeted RNA recombination method described previously, using MHV mutant Alb4 or Alb1 as the recipient virus (21, 28). In some earlier experiments, donor RNA was cotransfected into cells along with recipient viral genomic RNA by using DEAE-dextran, and resulting progeny virus was thermally inactivated at 40°C for 24 h to select recombinants (21). In most experiments, donor RNA was introduced into infected cells by electroporation, and released virus was subjected to plaque assay without heat treatment (28). Recombinants were plaque purified prior to further analysis.

**RNA purification, synthesis, and sequencing.** Virus was purified and viral genomic RNA was isolated exactly as described before (21). Total cytoplasmic RNA from MHV-infected 17Cl1 cell monolayers was purified by a Nonidet P-40-gentle lysis procedure (19). Synthetic transcripts from vectors truncated with *Nsi*I (pCK120) or *Hin*dIII (all other plasmids) were produced with bacteriophage T7 RNA polymerase as described previously (27), except that RNA products were purified with RNaid (Bio 101, Inc.). Direct RNA sequencing was performed by a modification of a dideoxy chain termination procedure (10, 33).

TABLE 1. Oligonucleotides used in plasmid construction

| Oligonucleotide | Sense | Purpose |
|---|---|---|
| PM171 (5′ ATGGTATGATGAACATGTCTCCAAAACCACAAAGACAAAGAGGT 3′) | + | *Bst*XI-*Acc*I linker for construction of pCK120 |
| PM172 (5′ CTACCTCTTTGTCTTTGTGGTTTTGGAGACATGTTCATCATACCATCCTT 3′) | − | *Bst*XI-*Acc*I linker for construction of pCK120 |
| PM179 (5′ TACGAATTCCCGGGATC 3′) | + | SOE PCR primer for construction of pB11; crosses vector *Bam*HI site |
| PM180 (5′ AAAAGACATCCTTAAAGTTT 3′) | − | SOE PCR primer for construction of pB11; forms MHV leader–BCV N gene junction |
| PM181 (5′ AAACTTTAAGGATGTCTTTT 3′) | + | SOE PCR primer for construction of pB11; forms MHV leader–BCV N gene junction |
| PM182 (5′ TTTGCTTGGGTTGAGCTC 3′) | − | SOE PCR primer for construction of pB11; crosses BCV N gene *Sac*I site; PCR primer for construction of pTM1 |
| PM186 (5′ TATCAACAACAAGATGGTATGATGAA 3′) | + | *Nsi*I-*Afl*III linker for construction of pB20 |
| PM187 (5′ CATGTTCATCATACCATCTTGTTGTTGATATGCA 3′) | − | *Nsi*I-*Afl*III linker for construction of pB20 |
| PM194A (5′ CCGCGGATCCAAGGATGTCTTTTACTCC 3′) | + | PCR primer for construction of pTM1 |
| PM112 (5′ CCATGATCAACTTCATTC 3′) | − | First-strand cDNA primer and PCR primer for cloning of recombinant N genes |
| PM148 (5′ ATCTTGTGGTTAATGTGG 3′) | + | PCR primer for cloning of recombinant N genes |

**Cloning and sequencing of chimeric N genes.** Chimeric N genes from mutants generated by targeted recombination were cloned from infected cellular RNA by reverse transcription followed by PCR using primers PM112 and PM148 (Table 1). The *Kpn*I-*Sac*I fragment obtained from each PCR product, running from the middle of the M gene to nearly the end of the 3′ untranslated region, was cloned into the *Kpn*I and *Sac*I sites of the vector pGEM-7Zf(+) (Promega). Alternatively, PCR products were ligated directly into a TA cloning vector (Invitrogen) per the manufacturer's instructions, except that the PCR fragment was gel purified with Geneclean (Bio 101, Inc.) prior to ligation. For each mutant, the DNA sequence of the cloned chimeric N gene was determined at least once in both directions. Final confirmation of BCV-MHV junctions was carried out by direct sequencing of purified genomic RNA (10, 33). DNA sequencing was performed by the method of Sanger et al. (36) using modified T7 DNA polymerase (Sequenase; U.S. Biochemical) and primers described elsewhere (31).

**In vivo labeling of virus-infected cells.** Wild-type, Alb4, and chimeric N mutant viruses were used to infect 17Cl1 cells in 20-$cm^2$ dishes at 37°C. After 6 h of infection, cells were washed with and incubated in methionine-free minimal essential medium for 1.5 h and then were labeled for 45 min with 1 ml of methionine-free minimal essential medium containing 25 μCi of [$^{35}$S]methionine. Monolayers were lysed with 100 μl of immunoprecipitation buffer (10 mM Tris-HCl [pH 7.5], 150 mM NaCl, 1 mM EDTA, 0.25% Nonidet P40, 0.2 mg of phenylmethylsulfonyl fluoride per ml, 0.01% sodium azide), and nuclei were removed by centrifugation. Equal portions of each sample were immunoprecipitated with anti-N antibodies and analyzed by sodium dodecyl sulfate-polyacrylamide gel electrophoresis (SDS-PAGE). Rabbit polyclonal antiserum raised against a peptide corresponding to amino acid residues 423 to 434 of the MHV-A59 N protein (VSRELTPEDRSL) was kindly provided by Kathryn Holmes (Uniformed Services University of the Health Sciences).

## RESULTS

**Interchange of a portion of spacer B of the N proteins of BCV and MHV.** As a first attempt to exchange parts of heterologous N molecules, we focused on a segment of the MHV N protein known to tolerate considerable sequence variation among different strains and mutants of MHV. The 25-amino-acid stretch that we have designated spacer B separates the acidic, highly conserved carboxy-terminal domain III of the MHV N protein from the remainder of the molecule, which is quite basic (31). In the N gene mutant Alb4, a deletion excising this region plus four flanking residues renders the virus temperature sensitive and thermolabile, such that it forms tiny plaques at the nonpermissive temperature (39°C) and has virions that are orders of magnitude more susceptible than the wild type to inactivation by incubation at the nonpermissive temperature (21). Thus, the absence of spacer B is not lethal but severely impairs N protein function under restrictive conditions.

We used targeted recombination to restore to Alb4 a mutant version of spacer B in which the first half of this region was replaced by a sequence encoding the corresponding part of the BCV N protein (Fig. 1). This was accomplished by altering plasmid pCK70, which serves as an in vitro transcription template for RNA7, the smallest of the MHV subgenomic RNAs (21). The *Bst*XI-*Acc*I fragment of pCK70 was replaced with a fragment made from synthetic oligonucleotides that encoded the BCV protein sequence and also contained an *Afl*III site not found in either the MHV or the BCV gene sequence. Substituted RNA7 transcribed from the resulting vector, pCK120, was cotransfected with Alb4 genomic RNA into cells, and recombinants were selected as progeny virus that survived heat selection and were able to form large (wild-type size) plaques at the nonpermissive temperature. Eight purified candidate recombinants were analyzed by PCR analysis of reverse transcripts of the distal portion of the N gene, and all were found to contain the BCV substitution, since they had restored the 87 bases missing from Alb4 and also had obtained the engineered *Afl*III site. The presence of the BCV sequence in one of these mutants, Alb85, was subsequently confirmed by sequencing of purified genomic RNA (data not shown). SDS-PAGE analysis of [$^{35}$S]methionine-labeled virions of Alb85 revealed that its

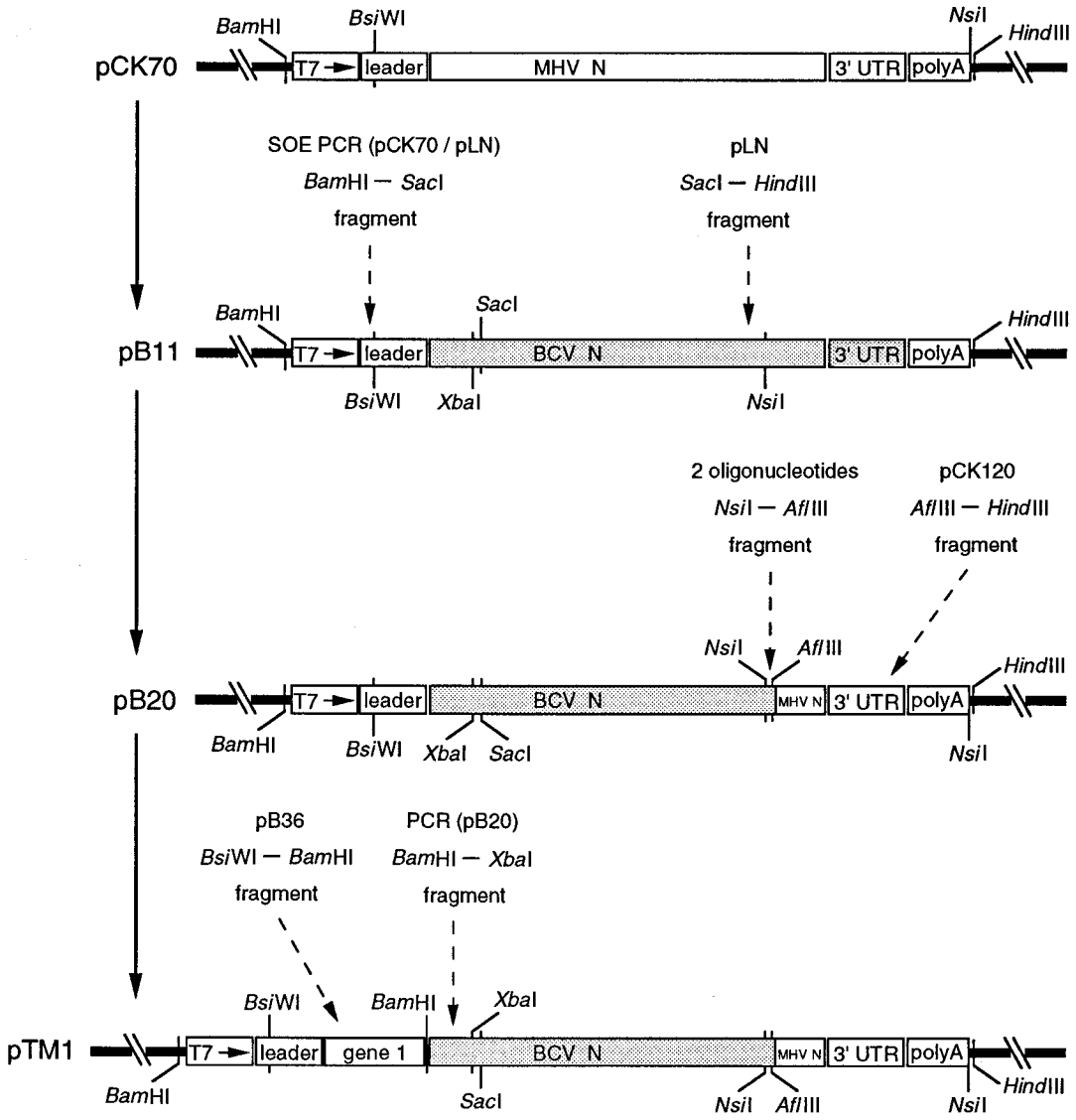


FIG. 2. Construction of a transcription vector, pTM1, used for synthesis of MHV DI RNA containing a portion of the BCV N coding region running from the amino terminus through spacer B. Restriction sites shown are relevant to the construction of pTM1 or intermediates, as detailed in Materials and Methods. The BCV sequence is shaded; all other segments are derived from MHV or vector elements. UTR, untranslated region.

chimeric N protein migrated slightly faster than wild-type MHV N protein, and it was labeled more intensely than wild-type N (within equivalent amounts of total virion protein) owing to the presence of additional methionine residues (Fig. 1). The apparent wild-type phenotype of Alb85 demonstrated that multiple substitutions of nonsimilar amino acids in spacer B had no effect on N protein function within an otherwise isogenic virus, extending the conclusion previously drawn on the basis of sequence comparison of the N proteins of a number of MHV strains (31).

**N protein recombination to the amino-terminal side of the spacer B region.** We next sought to introduce significantly larger portions of the BCV N gene into the MHV genome. For this purpose we constructed an MHV DI transcription vector, pTM1, containing all of the BCV N coding region located to the amino-terminal side of the sequence that had been successfully incorporated into Alb85 (Fig. 2). Thus, pTM1 encoded a chimeric N protein comprising domain I, spacer A, domain II, and part of spacer B of BCV N, followed by the remainder of spacer B and domain III of MHV N. This approach (i.e., the retention of the MHV N domain III) was taken initially because domain III is one of the most divergent regions between the two N proteins (see Fig. 6A). We expected that recombinants would arise by single crossover events exchanging the 3′ end of donor DI RNA for the corresponding region of the recipient genome RNA. Hence, if exchange of the BCV domain III and MHV domain III were functionally unallowed, detection of allowed substitutions elsewhere in the molecule would likely be precluded. Later experiments indicated that this assumption was valid.

Unlike earlier targeted recombinations (Fig. 1) (21, 33, 44), those with pTM1 were not expected to have a single defined product. Although the right (BCV-MHV) boundary of a resulting recombinant N gene would be determined by the junction constructed in the spacer B region of the vector, the left (MHV-BCV) boundary would be determined by the locus of

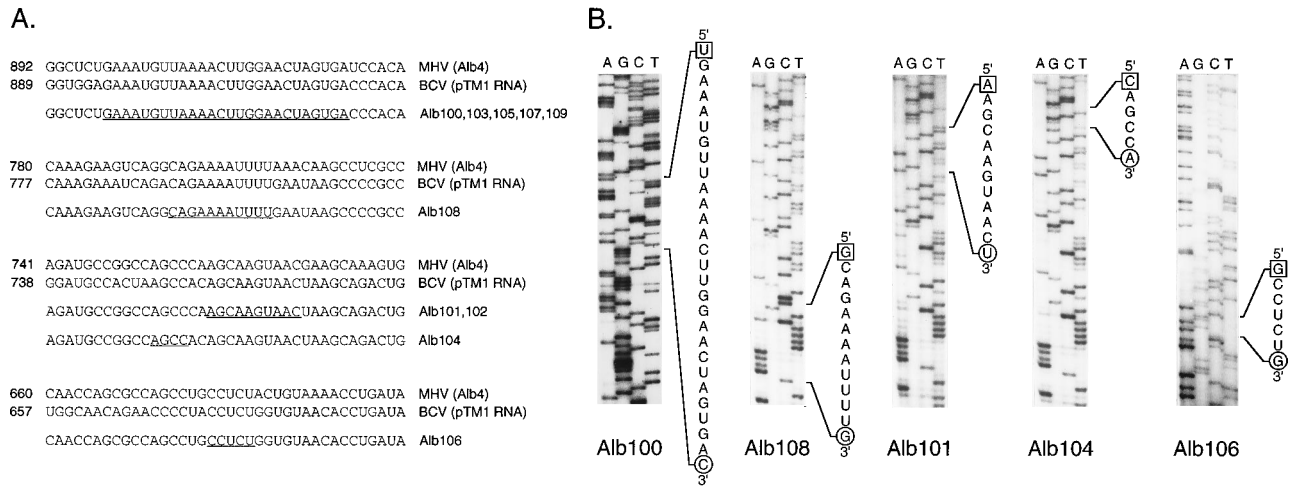


FIG. 3. Nucleotide sequences of the crossover junctions of MHV-BCV chimeric N mutants Alb100 to Alb109 obtained with pTM1 donor RNA. (A) The junction sequence of each recombinant, or set of recombinants, is shown beneath an alignment of the corresponding portions of the MHV and BCV N gene sequences. Numbering begins with the start of each respective N coding region. The region of sequence common to MHV and BCV in which the crossover event occurred is underlined. (B) Sequence of the crossover junction of genomic RNA isolated from purified virus for one member of each class of recombinant. The indicated segments of sequence are given as positive-sense RNA. The first flanking base unique to MHV or BCV is squared or circled, respectively.

the crossover event, which, in principle, might occur at any one of various points. In multiple independent experiments, Alb4-infected L2 cells were transfected with pTM1-derived DI RNA, and recombinants were identified as progeny virus able to form large plaques at 39°C. Nine independent recombinants, designated Alb100, Alb101, and Alb103 to Alb109, were isolated in this search. An additional recombinant, Alb102, potentially a sibling of Alb101, was also retained for further analysis because it formed intermediate-size plaques, rather than large plaques. Except for Alb102, no phenotypic differences by comparison with the wild type were noted in the growth or plaque forming ability of any of the mutants. The entire N gene of each mutant was cloned and sequenced to determine the exact location of its crossover and whether it harbored other mutations or multiple crossovers. Final confirmation of each crossover junction was then obtained by sequencing genomic RNA purified from each recombinant virus. These results are summarized in Fig. 3. As had been expected if recombinants were generated by a single crossover, the N genes of Alb100 to Alb109 had identical 3′ termini, including the right (BCV-MHV) boundary that had been engineered into the vector pTM1. Each had a single left (MHV-BCV) boundary, and there were no additional mutations with respect to the two parent sequences. Five different crossover sites were obtained at the left boundaries, ranging from bases 677 to 923 (MHV N coding region coordinates). One of these had been independently isolated five times (Alb100, Alb103, Alb105, Alb107, and Alb109); the other sites were represented by one independent isolate each (Alb101, Alb104, Alb106, and Alb108). The mutant with a variant plaque size, Alb102, was found to have an N gene sequence identical to that of Alb101, indicating that its plaque size phenotype must map elsewhere in the genome.

The mutant containing the largest extent of the BCV sequence, Alb106, had a crossover junction between bases 677 and 681 (MHV N coding region coordinates), falling at a point midway through the N molecule, or in the first third of domain II (see Fig. 6B). To determine whether this represented a maximal limit for the left boundary of this type of recombinant, additional targeted recombinations were attempted with donor RNA from pTM1, but using Alb1 as the recipient virus instead of Alb4. The N gene mutant Alb1, like Alb4, is temperature sensitive and thermolabile. It contains two point mutations, at bases 368 and 378, the second of which is responsible for its phenotype; at the protein level, these fall in the latter part of domain I of the N molecule (28). The use of this mutant as a recipient virus was intended to force selected recombination events to occur prior to base 378, and hence, well to the left of the crossover junction of Alb106. However, in a number of targeted recombination experiments we were unable to obtain recombinants with Alb1 as the recipient and pTM1 RNA as the donor. The results from one such set of transfections are shown in Table 2. To rule out the possibility that factors other than the BCV sequence of pTM1 caused this negative result, control transfections were carried out at the same time using DI RNA from the vector pB36, which contains only MHV components. In contrast with pTM1 RNA, pB36 RNA consis-

TABLE 2. Ability to detect recombinants with Alb1 as recipient[a]

| Vector and amt of DI RNA (μg) | Titer (PFU/ml) at 39°C | |
|---|---|---|
| | Small plaques | Large plaques |
| None | | |
| 0 | $3.6 \times 10^6$ | ND[b] |
| 0 | $3.3 \times 10^6$ | ND |
| pTM1 | | |
| 0.5 | $3.2 \times 10^6$ | ND |
| 1.0 | $3.6 \times 10^6$ | ND |
| 2.0 | $5.6 \times 10^6$ | ND[c] |
| pB36 | | |
| 0.5 | $5.9 \times 10^5$ | $2.3 \times 10^3$ |
| 1.0 | $8.4 \times 10^5$ | $1.8 \times 10^3$ |
| 2.0 | $3.6 \times 10^5$ | $2.1 \times 10^3$ |

[a] Alb1-infected L2 cells were transfected with the indicated DI RNA (or $H_2O$ as control) and plated onto 17Cl1 monolayers. Progeny virus titers were determined on L2 cells.

[b] ND, not detected.

[c] In one sample, large plaques were detected at a titer of $2.7 \times 10^3$ PFU/ml, but upon sequence analysis these were found to be revertants of Alb1 (data not shown).

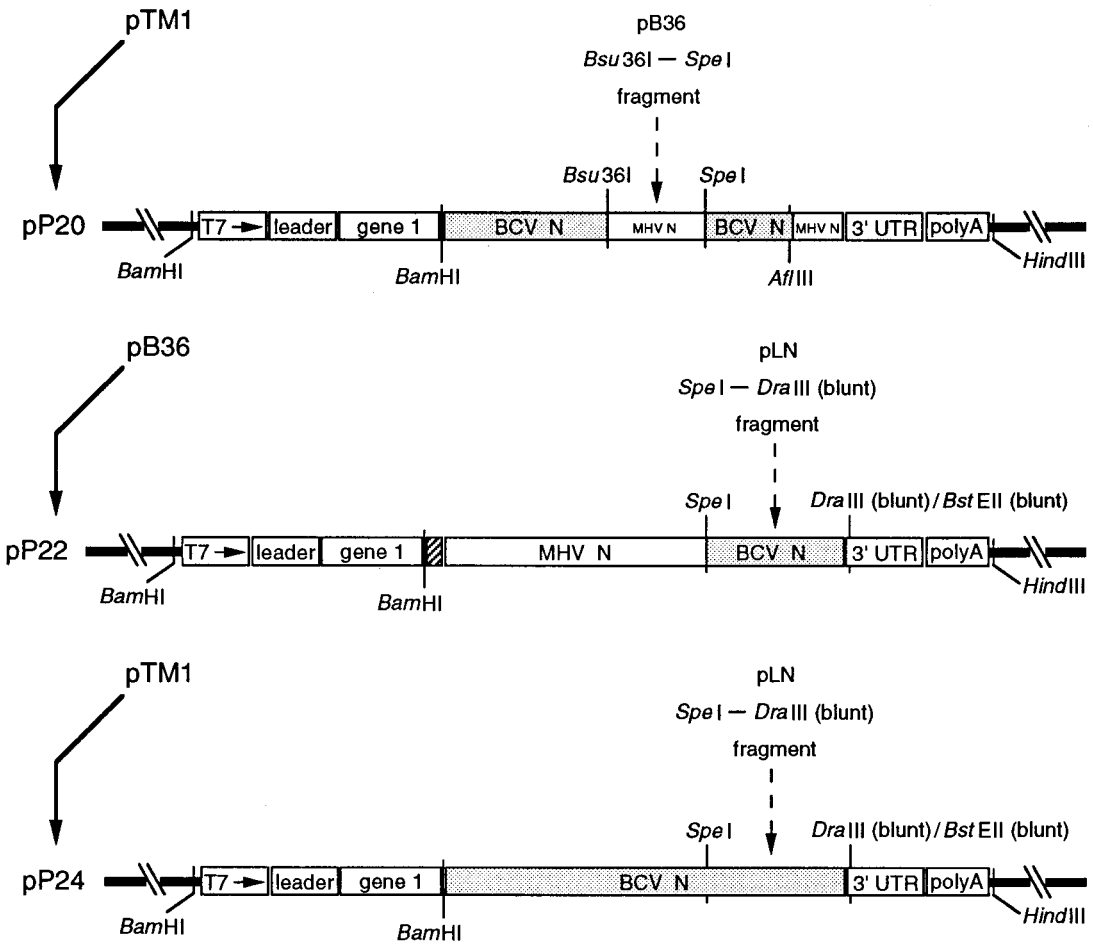


FIG. 4. Construction of additional transcription vectors used for synthesis of MHV DI RNAs containing chimeric MHV-BCV N coding regions. Relevant restriction sites are shown for each, as detailed in Materials and Methods. Plasmid pP20 contains the same extent of the BCV sequence as pTM1, except that the SR-rich region of N has been replaced with that of MHV. pP22 contains the latter portion of domain II as well as all of spacer B and domain III of the BCV N gene. pP24 contains the entire BCV N gene. The BCV sequence is shaded; all other segments are derived from MHV or vector elements. A short linker of a heterologous sequence used in construction of the parent vector of pP22, pB36 (28), is hatched. UTR, untranslated region.

tently gave rise to recombinants. This strongly implied that, beyond a certain point in domain II, the BCV N protein sequence is lethal in the context of the MHV N protein.

**Other N protein substitutions.** Comparison of the BCV and MHV N proteins suggested that the limiting boundary encountered by Alb106, the most extensive chimeric mutant, was a serine- and arginine-rich (SR-rich) region that is the most divergent portion of domain II (see Fig. 6A). To test the possibility that this fragment of the N protein was the determinant restricting exchange between the MHV and BCV N proteins, we constructed a vector, pP20, that was identical to pTM1, except that the MHV N SR-rich region had been restored in place of that of BCV (Fig. 4).

Two additional constructs were also made (Fig. 4). Vector pP22, designed to test the exchangeability of domain III, contained the allowed portion of domain II and all of domain III of the BCV N gene. Vector pP24, containing the entire BCV N coding region, was designed in consideration of the possibility that interacting regions of the N protein could be interchanged only coordinately. Neither of the latter two vectors yielded recombinants with Alb1 or Alb4 as the recipient, in contrast with pB36 controls, which gave large-plaque-forming recombinants at relatively high efficiency (data not shown). On the basis of this, we concluded that exchange of the carboxy-terminal domain III between MHV and BCV was unallowed. It should be noted that, in both pP22 and pP24, the new junction generated by the joining of the blunted *Dra*III site of the BCV clone segment to the blunted *Bst*EII site of the MHV clone segment created a 6-base deletion and four single-base substitutions with respect to the authentic MHV sequence in the 30 bases immediately downstream of the N gene stop codon (Fig. 4). We have previously shown that this region is tolerant to a 5-base insertion (at the *Bst*EII site) in a recombinant virus (21). However, at this time we cannot strictly rule out the possibility that the failure to obtain MHV recombinants with pP22 and pP24 was due to constraints at the level of the sequence composition of the 3′ untranslated region, rather than the allowed amino acid composition of the carboxy terminus of the N protein.

Targeted recombination between pP20-derived DI RNA and Alb1 gave rise to two independent large-plaque-forming candidates, Alb112 and Alb113. The N genes of these viruses were analyzed by the same criteria as those applied to the preceding set of recombinants, and the results are shown in Fig. 5. The left crossover junctions of both Alb112 and Alb113 were located very close to each other and to the Alb1 mutations. Remarkably, the crossover that generated Alb112 occurred at a single nucleotide (base 367 of the MHV N coding

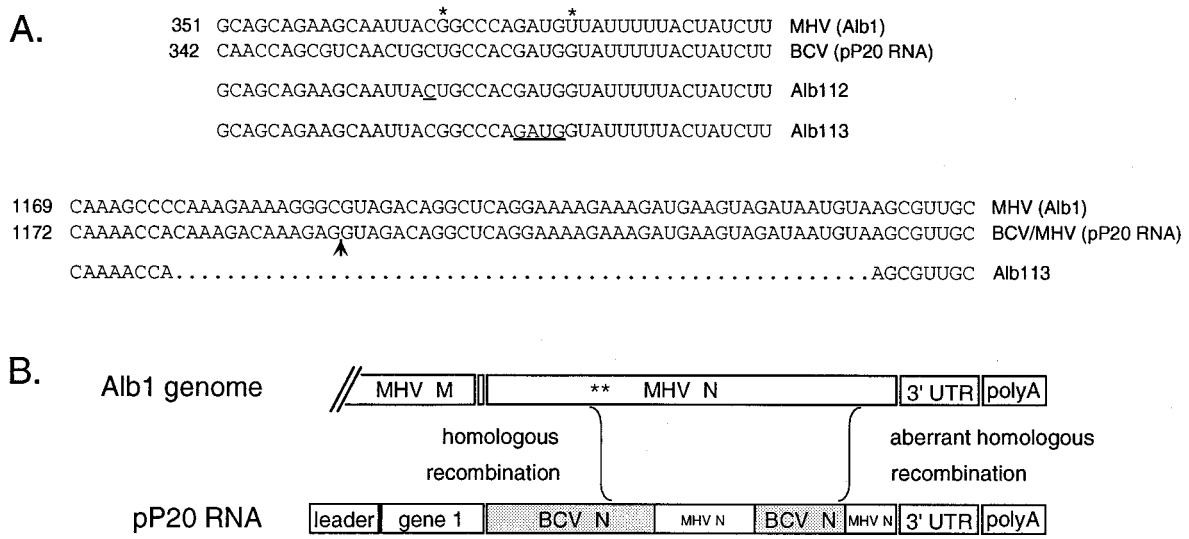


FIG. 5. Crossover junctions of MHV-BCV chimeric N mutants Alb112 and Alb113 obtained with pP20 donor RNA. (A) Crossover junction nucleotide sequences. In the upper set, the sequence of each recombinant is shown beneath an alignment of the corresponding portions of the MHV and BCV N gene sequences. Numbering begins with the start of each respective N coding region. The region of the sequence common to MHV and BCV in which the crossover event occurred (a single base in the case of Alb112) is underlined. The two bases in the MHV Alb1 mutant that differ from those in the wild type are indicated (asterisks); only the second of these is responsible for the Alb1 temperature-sensitive phenotype (28). In the lower set, the deletion in Alb113 is shown beneath an alignment of the corresponding portions of the MHV N gene and the donor chimeric RNA from pP20. The junction between BCV and MHV sequence in pP20 RNA is indicated (arrowhead). (B) Two crossover events proposed to have given rise to Alb113. UTR, untranslated region.

region), immediately 5′ to the first of the two point mutations of Alb1. The crossover that generated Alb113 was immediately 5′ to the second (phenotypically relevant) Alb1 mutation. Thus, Alb113 retained the first (phenotypically silent) mutation of Alb1.

Alb112 was found to have the expected 3′ junction between the BCV and MHV sequences in spacer B, which was dictated by the composition of the donor RNA vector. Alb113, however, had a deletion of 54 nucleotides in this region, creating an 18-amino-acid in-frame deletion partially overlapping the spacer B region. Since it would have been highly improbable to have selected a recombinant that had also randomly acquired a large deletion in the same passage, we think it likely that Alb113 was actually generated by two crossover events (Fig. 5B). By the classification system put forward by Lai (25), the first of these (viewed from the 5′ direction) would have been a homologous recombination event occurring between the two Alb1 mutations; the second, which produced the deletion, would have been an aberrant homologous recombination event in the 3′ half of spacer B. Prior studies of recombination between two different strains of MHV have provided numerous examples of progeny genomes containing more than one crossover (18, 25).

Elsewhere in their N genes, Alb112 and Alb113 had the sequences determined by the vector pP20. That is, they contained the BCV sequence from the left crossover junction through the remainder of domain I, spacer A, domain II, and half of spacer B with the exception of a segment of the MHV sequence running from the left edge of the SR-rich region through the middle of domain II. There were no other mutations with respect to the parent sequences. This demonstrated that further replacement of the MHV N sequence by the BCV N sequence, proceeding into domain I, was allowed provided that the SR-rich region of MHV N was retained. Our results also suggested that the next barrier to sequence interchange was reached in the locus of the Alb1 mutations.

**Analysis of chimeric N proteins.** Figure 6A shows an alignment of the MHV and BCV N proteins. Nonhomology between the two sequences is concentrated in six places: the amino-terminal half of domain I (MHV residues 1 to 65), spacer A (residues 140 to 162), the SR-rich region (residues 194 to 227), the latter portion of domain II (residues 329 to 363), spacer B (residues 381 to 405), and domain III (residues 406 to 454). The collection of recombinants we have isolated (summarized in Fig. 6B) demonstrates that three of these regions, as well as the flanking sequence, can be replaced in MHV N by their BCV N counterparts. To examine the expression of the N proteins of these chimeric mutants in comparison with wild-type MHV N protein, we labeled virus-infected cells with [$^{35}$S]methionine and immunoprecipitated N proteins with an antipeptide antibody directed against part of domain III, which all of them have in common. As shown in the SDS-PAGE analysis in Fig. 6C, all of the recombinants synthesized comparable amounts of N protein. Many of the chimeric N proteins (those of Alb100, Alb108, Alb101, Alb102, Alb104, and Alb106) migrated slightly faster than wild-type MHV N, despite being slightly larger. The SDS-PAGE mobilities of Alb112 and Alb113, however, were the most aberrant, causing them to appear some 3 to 4 kDa larger than they were predicted to be on the basis of the primary sequence. This higher apparent molecular weight has been observed previously for the N proteins of some of the strains of MHV (MHV-1, MHV-S, and MHV-JHM) (6, 32). The data in Fig. 6, taken together with previous results (31), now allow us to assign this attribute to the sequence composition of spacer A. It is possible that some variants of spacer A undergo a unique posttranslational modification or, alternatively, that some spacer A sequences lend to a portion of the N molecule a residuum of secondary structure that is not denatured by SDS. It is not presently clear whether this property of spacer A has any significance for N protein function.

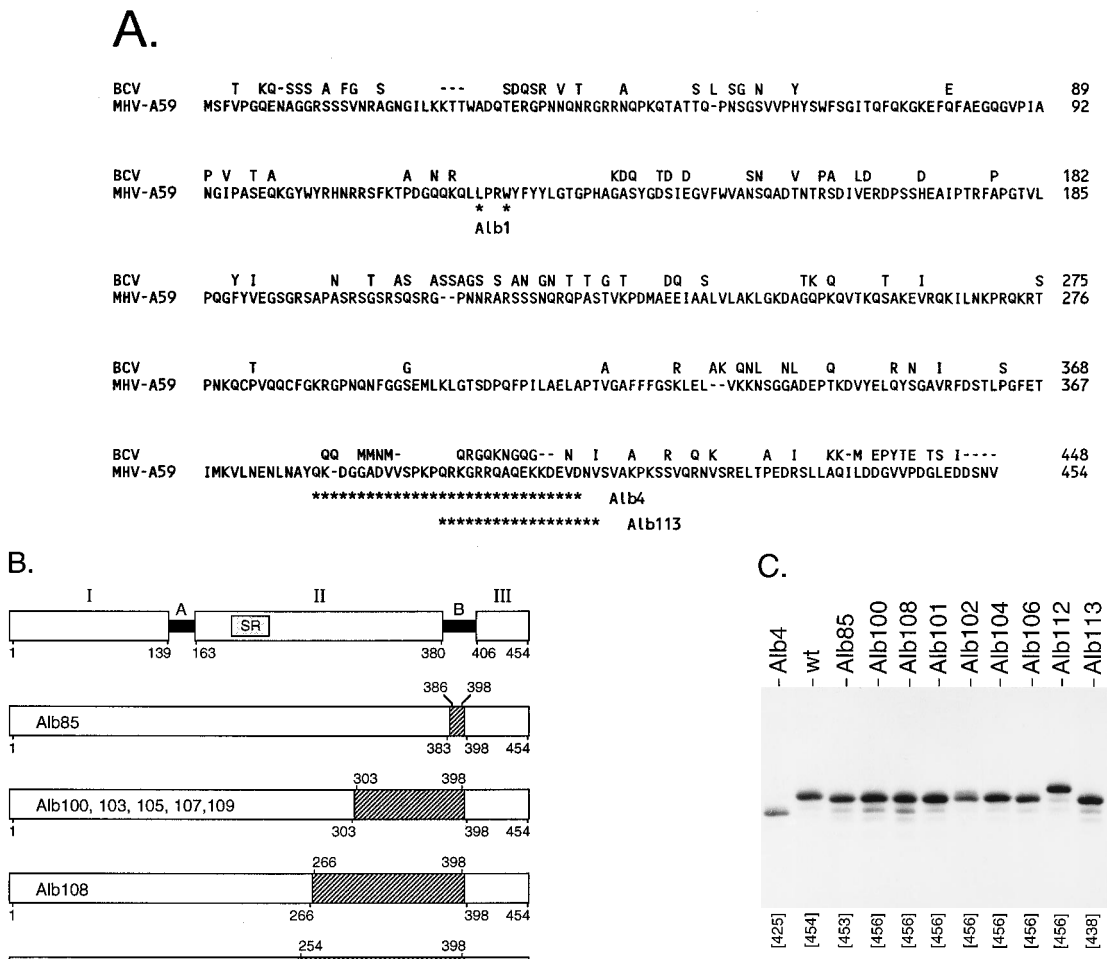


FIG. 6. N proteins of all MHV-BCV chimeric mutants. (A) Comparison of the BCV and MHV-A59 N proteins. A pairwise alignment of the two amino acid sequences was obtained by using the GAP and BESTFIT programs of the Genetics Computer Group software (12) and modified according to an alignment including the N proteins of eight other serotypes of MHV. Only those BCV residues that are different from MHV residues are shown. Dashes indicate gaps. The two point mutations in Alb1 and the deletions in Alb4 and Alb113 are indicated (asterisks). (B) Summary of all recombinant N proteins obtained in this study. At the top is a previously proposed model of the N protein consisting of three domains separated by two spacer regions (31); the SR-rich region of domain II is indicated. BCV-derived portions are shaded; the remaining portions are MHV derived. BCV and MHV residue numbers are given above and below each protein, respectively. (C) Electrophoretic analysis of mutant Alb4, wild-type (wt), and recombinant N proteins. Infected 17Cl1 cells were labeled with [$^{35}$S]methionine from 7.5 to 8.25 h postinfection, and N proteins were immunoprecipitated and analyzed by SDS-PAGE followed by fluorography. The number of amino acid residues in each N variant is indicated below.

## DISCUSSION

This study was initiated to learn what regions of the MHV N protein could be interchanged with their BCV counterparts as a means of probing N structure and function. Homologous, but significantly different portions of the N gene coding sequence from BCV were introduced into the MHV genome in place of the corresponding segments of the MHV N coding sequence. The resulting N mutants all behaved like wild-type MHV, suggesting that the substituted regions are functionally compatible in these two viruses. It should be noted that, although the BCV N gene was specifically used in these experiments, the BCV N sequence is almost identical to those of human coronavirus OC43 (17) and turkey coronavirus (45). Our results have shown that some portions of the N protein (including most of domain II, the RNA-binding portion of N) have been functionally conserved across these different species, whereas some portions have diverged too far to be functionally equivalent. We have thus identified regions to focus upon in future mutagenesis experiments. Of the six most divergent parts of the protein (Fig. 6A), three can be exchanged between BCV and MHV: spacer A, the latter portion of domain II, and spacer B. In contrast, we were unable to transfer from BCV to MHV the other three most divergent segments: the amino-terminal half of domain I, the SR-rich region, and domain III.

In the case of the amino terminus of domain I, it is possible that inability to obtain transfer was restricted by the amount of flanking sequence in the donor RNA vector. For the SR-rich region and domain III, however, failure to transfer cannot have been due to this factor, and we are led to conclude that stable recombinants were selected against at the level of protein function.

That transfer of some N protein regions was not allowed could suggest that these are segments of the molecule that interact with other viral components (including other parts of the N molecule) or with host cell components. The latter possibility is argued against by the near-identity of the BCV, human coronavirus OC43, and turkey coronavirus N genes. It seems unlikely that there would be an N-associating host-specific factor common to bovine, human, and avian cells but absent from murine cells. Thus, it is more feasible that the portions of N that cannot be transferred between species are involved in associations with other viral proteins. An attractive possibility is that one mode of N monomer-monomer interactions is a head-to-tail linkage between the highly basic amino terminus (domain I) of one molecule and the acidic carboxyl terminus (domain III) of another.

Among the nonexchangeable segments of the N protein, the SR-rich region is most intriguing. In MHV this consists of an island of 34 residues (amino acids 194 to 227) containing 11 serines and 7 arginines. The corresponding region of BCV N has a similar composition but a highly varied primary sequence (Fig. 6A). In fact, among all coronavirus N proteins this region is highly divergent, yet a core motif of SRXXSRXXSR can be found within each. The SR-rich region of N is reminiscent of the SR (or RS) domains found in a large number of RNA-binding proteins, many of which are involved in pre-mRNA splicing (1, 22, 46). Current evidence suggests that SR domains do not directly participate in RNA binding but mediate protein-protein interactions and are the targets for phosphorylation by protein kinases. We do not yet know the extent or significance of the resemblance between N and these proteins.

In addition to contributing to our understanding of the MHV N protein, the present study allows some interesting conclusions about coronavirus recombination. The work reported here clearly demonstrates that targeted recombination can be used to make extensive substitutions in the coronavirus genome, generating recombinants that could not be made otherwise between two viruses separated by a species barrier. Previous site-specific mutations made by this technique were limited to point mutations or a small insertion (21, 33, 44). Besides the extent of sequence change created, a further property of most members of the present set of mutants was that their crossover boundaries were determined by the selective pressures of the experimental system. In addition, the results of this study provide a reminder of the plasticity of RNA genomes. Of the 13 mutants generated for this work, two had unintended secondary mutations: a substantial deletion in Alb113 and an unmapped mutation outside the N gene that caused a variant plaque size phenotype in Alb102. While we cannot rule out the possibility that the deletion in Alb113 arose independently or that it was generated by T7 RNA polymerase in the donor RNA, the most likely explanation of its origin is that it resulted from a secondary crossover event in the same round of replication that created its chimeric boundary in domain I of the N gene (Fig. 5B). The secondary mutation in Alb102, however, probably cannot be attributed to a recombination-associated event.

RNA recombination is thought to occur via a template switching or copy choice mechanism wherein the replicating polymerase pauses and transfers its newly synthesized RNA strand to a different template, upon which it resumes synthesis (3, 4, 16, 20). This may occur by the polymerase dissociating from the first template and hopping to a second (25), or it may result from a processive mechanism which does not require polymerase dissociation (15). Previous studies of MHV recombination have shown that selective pressures can create the appearance of preferred sites of recombination (2), but, at least for one region examined in detail, recombination is close to random in the absence of selection (3). Globally, the rate of MHV recombination is constant enough for the construction of a classical genetic map (4), but more precise analysis has revealed an increasing gradient of recombination rates (in the 5′-to-3′ direction) across the length of the genome (11). Five of the twelve independently isolated MHV-BCV chimeric mutants reported here (Alb100, Alb103, Alb105, Alb107, and Alb109) had crossovers occurring within the longest stretch of exact homology between the MHV and BCV N genes (26 nucleotides, bases 898 to 923 [Fig. 3A]). However, we do not believe that this supports the notion that recombination is favored within extended regions of homology or that this represents a recombinational hot spot within the N gene. We did not isolate any recombinants having crossovers within two other long stretches of exact homology, one equally large (bases 865 to 890) and one slightly smaller (bases 1111 to 1133). In contrast, crossovers were obtained in regions of only 1 (Alb112), 4 (Alb104 and Alb113), or 5 (Alb106) nucleotides of exact homology (Fig. 3A and 5A). This is consistent with the idea that, during template switching, the base pairing that anchors the nascent RNA strand to the acceptor template can be physically distant from the site at which the crossover occurs (25). Examples of coronavirus (3) and picornavirus (20) recombinants in which there is no sequence identity at the point of crossover have been found previously. Within our mutant set, selection is most likely the overriding factor in any apparent bias in the distribution of crossover sites. Although all the chimeric MHV-BCV mutants were selected to have a wild-type phenotype, we have previously shown that selection between two phenotypically wild-type viruses differing at only a single amino acid in the N gene can be very subtle but complete (33).

Coronaviruses display strong host species specificities (38, 42). A major component (and, perhaps, the only component) of this restriction operates at the level of virus-receptor interactions (8). Thus, there is a constraint on the evolutionary distance over which interstrain recombination could naturally occur. Our experiments have rigged an artificial situation that, among other things, pushed the limit of the degree of sequence divergence upon which coronavirus RNA recombination could act. We have shown that viable progeny could be isolated from two parental RNA species that diverged by 30% in nucleotide sequence. Moreover, the frequency at which these recombinants arose did not differ markedly from that obtained with control isogenic donor RNA. These results contrast with the observation that, for picornaviruses, intertypic recombination is much less easily observed than intratypic recombination (25). Thus, intertypic recombinants between Mahoney type 1 poliovirus and Lansing type 2 poliovirus, which are 15% divergent in nucleotide sequence, were obtained at a more than 100-fold lower frequency than type 1 intratypic recombinants (20). On the basis of our current picture of the mechanism of RNA recombination, it is not clear whether this drop in frequency is inherent in the divergence of nucleotide sequences or whether it reflects a reduced ability of RNA templates of the two types to colocalize during viral RNA synthesis.

A more striking contrast is seen between what we have found to be allowed in coronavirus RNA recombination and what is clearly unallowed in DNA recombination. For both

prokaryotes and eukaryotes, there has accumulated evidence that the nature of the barrier to genetic exchange between species is recombination itself (29, 34, 37). Thus, for the closely related species *E. coli* and *Salmonella typhimurium*, a genomic sequence divergence of 16% directly presents an obstacle that reduces the frequency of DNA recombination some $10^5$ fold. This restriction operates, in large part, at the level of mismatch repair. The ability of RNA recombination to proceed effectively with sequences diverging by 30% underlines the fundamental mechanistic differences between these two processes. More significantly, it emphasizes the potential importance of RNA recombination as a driver of coronavirus evolution.

## ACKNOWLEDGMENTS

We are grateful to Savithra Senanayake and David Brian for providing the BCV N gene clone pLN, to Kay Holmes for anti-N antisera, and to Dilip Nag for enlightening discussions. We thank Tim Moran of the Molecular Genetics Core Facility of the Wadsworth Center for the synthesis of oligonucleotides.

This work was supported in part by Public Health Service grant AI 31622 from the National Institutes of Health.

## REFERENCES

1. **Amrein, H., M. L. Hedley, and T. Maniatis.** 1994. The role of specific protein-RNA and protein-protein interactions in positive and negative control of pre-mRNA splicing by *transformer 2*. Cell **76:**735–746.
2. **Banner, L. R., J. G. Keck, and M. M. C. Lai.** 1990. A clustering of RNA recombination sites adjacent to a hypervariable region of the peplomer gene of murine coronavirus. Virology **175:**548–555.
3. **Banner, L. R., and M. M. C. Lai.** 1991. Random nature of coronavirus RNA recombination in the absence of selective pressure. Virology **185:**441–445.
4. **Baric, R. S., K. Fu, M. C. Schaad, and S. A. Stohlman.** 1990. Establishing a genetic recombination map for murine coronavirus strain A59 complementation groups. Virology **177:**646–656.
5. **Baric, R. S., G. W. Nelson, J. O. Fleming, R. J. Deans, J. G. Keck, N. Casteel, and S. A. Stohlman.** 1988. Interactions between coronavirus nucleocapsid protein and viral RNAs: implications for viral transcription. J. Virol. **62:**4280–4287.
6. **Cheley, S., V. L. Morris, M. J. Cupples, and R. Anderson.** 1981. RNA and peptide homology among murine coronaviruses. Virology **115:**310–321.
7. **Compton, S. R., D. B. Rogers, K. V. Holmes, D. Fertsch, J. Remenick, and J. J. McGowan.** 1987. In vitro replication of mouse hepatitis virus strain A59. J. Virol. **61:**1814–1820.
8. **Compton, S. R., C. B. Stephensen, S. W. Snyder, D. G. Weismiller, and K. V. Holmes.** 1992. Coronavirus species specificity: murine coronavirus binds to a mouse-specific epitope on its carcinoembryonic antigen-related receptor glycoprotein. J. Virol. **66:**7420–7428.
9. **Décimo, D., H. Philippe, M. Hadchouel, M. Tardieu, and M. Meunier-Rotival.** 1993. The gene encoding the nucleocapsid protein: sequence analysis in murine hepatitis virus type 3 and evolution in *Coronaviridae*. Arch. Virol. **130:**279–288.
10. **Fichot, O., and M. Girard.** 1990. An improved method for sequencing of RNA templates. Nucleic Acids Res. **18:**6162.
11. **Fu, K., and R. S. Baric.** 1994. Map locations of mouse hepatitis virus temperature-sensitive mutants: confirmation of variable rates of recombination. J. Virol. **68:**7458–7466.
12. **Genetics Computer Group.** 1994. Program manual for the Wisconsin package, version 8. Genetics Computer Group, Madison, Wis.
13. **Hofmann, M. A., S. D. Senanayake, and D. A. Brian.** 1993. A translation-attenuating intraleader open reading frame is selected on coronavirus mRNAs during persistent infection. Proc. Natl. Acad. Sci. USA **90:**11733–11737.
14. **Horton, R. M., and L. R. Pease.** 1991. Recombination and mutagenesis of DNA sequences using PCR. *In* M. J. McPherson (ed.), Directed mutagenesis, a practical approach. IRL Press, New York.
15. **Jarvis, T. C., and K. Kirkegaard.** 1991. The polymerase in its labyrinth: mechanisms and implications of RNA recombination. Trends Genet. **7:**186–191.
16. **Jarvis, T. C., and K. Kirkegaard.** 1992. Poliovirus RNA recombination: mechanistic studies in the absence of selection. EMBO J. **11:**3135–3145.
17. **Kamahora, T., L. H. Soe, and M. M. C. Lai.** 1989. Sequence analysis of nucleocapsid gene and leader RNA of human coronavirus OC43. Virus Res. **12:**1–9.
18. **Keck, J. G., L. H. Soe, S. Makino, S. A. Stohlman, and M. M. C. Lai.** 1988. RNA recombination of murine coronaviruses: recombination between fusion-positive mouse hepatitis virus A59 and fusion-negative mouse hepatitis virus 2. J. Virol. **62:**1989–1998.
19. **Kingsman, S. M., and C. E. Samuel.** 1980. Mechanism of interferon action. Interferon-mediated inhibition of simian virus-40 early RNA accumulation. Virology **101:**458–465.
20. **Kirkegaard, K., and D. Baltimore.** 1986. The mechanism of RNA recombination in poliovirus. Cell **47:**433–443.
21. **Koetzner, C. A., M. M. Parker, C. S. Ricard, L. S. Sturman, and P. S. Masters.** 1992. Repair and mutagenesis of the genome of a deletion mutant of the coronavirus mouse hepatitis virus by targeted RNA recombination. J. Virol. **66:**1841–1848.
22. **Kohtz, J. D., S. F. Jamison, C. L. Will, P. Zuo, R. Lührmann, M. A. Garcia-Blanco, and J. L. Manley.** 1994. Protein-protein interactions and 5′-splice-site recognition in mammalian mRNA precursors. Nature (London) **368:**119–124.
23. **Kunita, S., M. Mori, and E. Terada.** 1993. Sequence analysis of the nucleocapsid protein gene of rat coronavirus SDAV-681. Virology **193:**520–523.
24. **Kunita, S., E. Terada, K. Goto, and N. Kagiyama.** 1992. Sequence analysis and molecular detection of mouse hepatitis virus using the polymerase chain reaction. Lab. Anim. Sci. **42:**593–598.
25. **Lai, M. M. C.** 1992. RNA recombination in animal and plant viruses. Microbiol. Rev. **56:**61–79.
26. **Lapps, W., B. G. Hogue, and D. A. Brian.** 1987. Sequence analysis of the bovine coronavirus nucleocapsid and matrix protein genes. Virology **157:**47–57.
27. **Masters, P. S.** 1992. Localization of an RNA-binding domain in the nucleocapsid protein of the coronavirus mouse hepatitis virus. Arch. Virol. **125:**141–160.
28. **Masters, P. S., C. A. Koetzner, C. A. Kerr, and Y. Heo.** 1994. Optimization of targeted RNA recombination and mapping of a novel nucleocapsid gene mutation in the coronavirus mouse hepatitis virus. J. Virol. **68:**328–337.
29. **Matic, I., C. Rayssiguier, and M. Radman.** 1995. Interspecies gene exchange in bacteria: the role of SOS and mismatch repair systems in evolution of species. Cell **80:**507–515.
30. **Nelson, G. W., and S. A. Stohlman.** 1993. Localization of the RNA-binding domain of mouse hepatitis virus nucleocapsid protein. J. Gen. Virol. **74:**1975–1979.
31. **Parker, M. M., and P. S. Masters.** 1990. Sequence comparison of the N genes of five strains of the coronavirus mouse hepatitis virus suggests a three domain structure for the nucleocapsid protein. Virology **179:**463–468.
32. **Parker, M. M., and P. S. Masters.** Unpublished data.
33. **Peng, D., C. A. Koetzner, and P. S. Masters.** 1995. Analysis of second-site revertants of a murine coronavirus nucleocapsid protein deletion mutant and construction of nucleocapsid protein mutants by targeted RNA recombination. J. Virol. **69:**3449–3457.
34. **Rayssiguier, C., D. S. Thaler, and M. Radman.** 1989. The barrier to recombination between *Escherichia coli* and *Salmonella typhimurium* is disrupted in mismatch-repair mutants. Nature (London) **342:**396–401.
35. **Sambrook, J., E. F. Fritsch, and T. Maniatis.** 1989. Molecular cloning: a laboratory manual, 2nd ed. Cold Spring Harbor Laboratory Press, Cold Spring Harbor, N.Y.
36. **Sanger, F., S. Nicklen, and A. R. Coulson.** 1977. DNA sequencing with chain terminating inhibitors. Proc. Natl. Acad. Sci. USA **74:**5463–5467.
37. **Selva, E. M., L. New, G. F. Crouse, and R. S. Lahue.** 1995. Mismatch correction acts as a barrier to homeologous recombination in *Saccharomyces cerevisiae*. Genetics **139:**1175–1188.
38. **Siddell, S., H. Wege, and V. Ter Meulen.** 1982. The structure and replication of coronaviruses. Curr. Top. Microbiol. Immunol. **99:**131–163.
39. **Siddell, S. G., A. Barthel, and V. Ter Meulen.** 1981. Coronavirus JHM: a virion-associated protein kinase. J. Gen. Virol. **52:**235–243.
40. **Stohlman, S. A., J. O. Fleming, C. D. Patton, and M. M. C. Lai.** 1983. Synthesis and subcellular localization of the murine coronavirus nucleocapsid protein. Virology **130:**527–532.
41. **Stohlman, S. A., and M. M. C. Lai.** 1979. Phosphoproteins of murine hepatitis virus. J. Virol. **32:**672–675.
42. **Sturman, L. S., and K. V. Holmes.** 1983. The molecular biology of coronaviruses. Adv. Virus Res. **28:**35–111.
43. **Tahara, S. M., T. A. Dietlin, C. C. Bergmann, G. W. Nelson, S. Kyuwa, R. P. Anthony, and S. A. Stohlman.** 1994. Coronavirus translational regulation: leader affects mRNA efficiency. Virology **202:**621–630.
44. **Van der Most, R. G., L. Heijnen, W. J. M. Spaan, and R. J. de Groot.** 1992. Homologous RNA recombination allows efficient introduction of site-specific mutations into the genome of coronavirus MHV-A59 via synthetic co-replicating RNAs. Nucleic Acids Res. **20:**3375–3381.
45. **Verbeek, A., and P. Tijssen.** 1991. Sequence analysis of the turkey enteric coronavirus nucleocapsid and membrane protein genes: a close genomic relationship with bovine coronavirus. J. Gen. Virol. **72:**1659–1666.
46. **Zahler, A. M., W. S. Lane, J. A. Stolk, and M. B. Roth.** 1992. SR proteins: a conserved family of pre-mRNA splicing factors. Genes Dev. **6:**837–847.